Rock and Soil Mechanics

Volume 44 | Issue 6 Article 4

10-3-2023

Characteristics of the cumulative plastic deformation and pore water pressure of saturated sand under cyclic intermittent loading

Qi YANG
School of Civil Engineering, Central South University, Changsha, Hunan 410075, China; Key Laboratory of Engineering Structures of Heavy Haul Railway of Ministry of Education, Central South University, Changsha, Hunan 410075, China, qiyang123@csu.edu.cn

Xiao-ya WANG
School of Civil Engineering, Central South University, Changsha, Hunan 410075, China

Ru-song NIE
School of Civil Engineering, Central South University, Changsha, Hunan 410075, China; Key Laboratory of Engineering Structures of Heavy Haul Railway of Ministry of Education, Central South University, Changsha, Hunan 410075, China, nierusong97@csu.edu.cn

Chen CHEN
School of Civil Engineering, Central South University, Changsha, Hunan 410075, China

See next page for additional authors

Recommended Citation

YANG, Qi; WANG, Xiao-ya; NIE, Ru-song; CHEN, Chen; CHEN, Yuan-zheng; and XU, Fang (2023) "Characteristics of the cumulative plastic deformation and pore water pressure of saturated sand under cyclic intermittent loading," *Rock and Soil Mechanics*: Vol. 44: Iss. 6, Article 4.
DOI: 10.16285/j.rsm.2022.6109
Available at: https://rocksoilmech.researchcommons.org/journal/vol44/iss6/4

Characteristics of the cumulative plastic deformation and pore water pressure of saturated sand under cyclic intermittent loading

Authors

Qi YANG, Xiao-ya WANG, Ru-song NIE, Chen CHEN, Yuan-zheng CHEN, and Fang XU

Rock and Soil Mechanics 2023 44(6): 1671−1682 ISSN 1000−7598
https: //doi.org/10.16285/j.rsm.2022.6109 http://rocksoilmech.researchcommons.org/journal

Characteristics of the cumulative plastic deformation and pore water pressure of saturated sand under cyclic intermittent loading

YANG Qi[1, 2], WANG Xiao-ya[1], NIE Ru-song[1, 2], CHEN Chen[1], CHEN Yuan-zheng[1], XU Fang[1, 2]
1. School of Civil Engineering, Central South University, Changsha, Hunan 410075, China
2. Key Laboratory of Engineering Structures of Heavy Haul Railway of Ministry of Education, Central South University, Changsha, Hunan 410075, China

Abstract: The long-term train loads can result in problems such as strength attenuation, excessive cumulative settlement and even subsidence in sandy soil foundations and filling materials, which can jeopardize train operation safety. To understand the mechanism of the disease, it is necessary to explore the cumulative plastic deformation and pore water pressure characteristics of saturated sand under intermittent loading. Therefore, dynamic triaxial tests under continuous and intermittent loading with different dynamic amplitudes and confining pressures were performed. The test results showed that: (1) The cumulative plastic deformation-loading cycle curve of saturated sand exhibited a "zigzag" pattern. The intermittent effect led to unloading rebound and significantly reduced the accumulated plastic deformation of sand in the later loading stage, which can transform the failure mode from "destructive" to "stable" under continuous loading. (2) For plastic stability and plastic creep, the pore water pressure-loading cycle curve showed a ladder shape. In the first dynamic loading stage, the pore water pressure increased rapidly with loading cycle while drainage occurred during the intermittent stage, causing pore water pressure was dissipated and approached or equaled zero, resulting in denser sand soil. In the subsequent loading stage, the cumulative amplitude of pore water pressure decreased significantly. For the incremental failure type, the pore water pressure increased rapidly and the specimen was damaged in the first loading stage. (3) A prediction model characterizing the two-stage development of cumulative plastic strain of sand under intermittent loading was established and its prediction effect was good. (4) Intermittent effect increased the resistance of sand to plastic deformation. The cumulative plastic strain of sand was overestimated and the dynamic strength was underestimated under continuous loading. The cumulative deformation characteristics and its mechanism of saturated sand under cyclic intermittent loading can be deeply understood.

Keywords: intermittent load of train; dynamic triaxial test; saturated sand; cumulative plastic deformation; excess pore water pressure

1 Introduction

In recent years, rapid development of rail transit systems, such as subways, high-speed railways, and heavy-haul railways, has led to various problems affecting the safety of train operations, including sand soil foundation, weakening filling strength[1], liquefaction[2−5], excessive cumulative settlement[6−9] and even subsidence due to long-term dynamic loading from trains. The dynamic mechanical characteristics (such as dynamic strength and elastic-plastic deformation) of saturated sand foundation and filling under train loading dominate the cumulative settlement of the roadbed and critical dynamic stress. This holds significant importance for the design, maintenance, and evaluation of railway substructures. Therefore, it is necessary to conduct research on the dynamic properties of saturated sandy soil under train loads.

The dynamic triaxial test is an effective means of simulating the stress state, physical properties, and boundary conditions of soil, and has become one of the important methods for studying the dynamic characteristics of soil[11]. Based on dynamic triaxial tests, global scholars have studied the effects of factors such as cyclic loading, confining pressure, consolidation ratio, and relative compactness on the strength and deformation characteristics as well as pore pressure of saturated sandy soil[12−17]. Liu et al.[18] studied the cumulative strain of gravelly soil under cyclic loading and found that its cumulative plastic strain increased with increasing initial static deviatoric stress and cyclic loading but decreased with increasing confining pressure, load frequency, and consolidation ratio. Chang et al.[19] investigated the dynamic characteristics of gravelly soil under traffic loads and pointed out that the stress−strain relationship of gravelly soil as a whole showed an increasing trend. The dynamic elastic modulus of gravelly soil showed a trend of sudden decrease followed by slight increase before decreasing again with increasing dynamic strain. Yilmaz et al.[20] evaluated the liquefaction sensitivity of various well-graded saturated fine sand soils through stress-controlled cyclic triaxial tests. They found that a single average particle size parameter was not sufficient to characterize the dynamic properties of sand soil. Sand

Received: 16 July 2022 Accepted: 14 December 2022
This work was supported by the National Natural Science Foundation of China (51878666, 51978672) and the Hangzhou Hub Engineering Construction Headquarters of China Railway Shanghai Group Co., Ltd. (2022-129, 2021-50).
First author: YANG Qi, male, born in 1982, PhD, Associate Professor, mainly engaged in teaching and research work in the field of ground and foundation. E-mail: qiyang123@csu.edu.cn
Corresponding author: NIE Ru-song, male, born in 1980, PhD, Associate Professor, mainly engaged in teaching and research work in railway subgrade and bridge pile foundation. E-mail: nierusong97@csu.edu.cn

soil with smaller pore ratio ranges was more susceptible to liquefaction even if their average particle sizes were the same. Pumphrey et al.[21], Tang et al.[22] and Salour et al.[23] have examined the influencing factors on the dynamic properties of sand subgrade and proposed models for predicting permanent deformation of subgrade.

In summary, continuous loading methods such as uninterrupted sine waves and semi-sine waves are mainly adopted in dynamic triaxial tests on sand soil to simulate train loads[24]. However, under actual train operating conditions, there is a certain interval of time between adjacent trains (generally not less than 5 minutes for high-speed trains, 10 minutes for heavy-haul railways, and 3 minutes for subways). Long-term dynamic loads on the subgrade and filling materials can be regarded as a combination of excitation during train passage and intermittence when there is no train. Therefore, to obtain the dynamic characteristics of the subgrade and filling materials under train loads more realistically, the loading intermittence caused by adjacent train operating intervals should be considered when simulating train dynamic loads in dynamic triaxial tests. Up to now, some scholars have conducted dynamic triaxial tests on soil under intermittent dynamic loads. Li et al.[25−26] and Nie et al.[27] employed a dynamic triaxial apparatus to explore the cumulative plastic strain, elastic strain, rebound modulus and excess pore water pressure of subgrade silt fillers under continuous and intermittent loadings. They proposed corresponding cumulative plastic strain prediction models and critical dynamic stress empirical formulas. Wang et al.[28] and Yildirim et al.[29] carried out a series of intermittent cyclic triaxial tests on soft clay soil, pointing out that the existence of intermittent stages leads to a significant decrease in the maximum residual strain and pore pressure generated in each stage during subsequent loadings. To date, the research objects mainly include silt, silty clay, and soft clay. Dynamic characteristics of sand soil under continuous uninterrupted cyclic loads have been systematically studied. However, dynamic triaxial tests on sand soil accurately simulating train intermittent loading characteristics are rare.

Hence, dynamic triaxial tests on saturated sand under continuous and intermittent loading conditions were carried out, considering different levels of dynamic stress and confining pressure. The dynamic characteristics of saturated sand under continuous and intermittent loading conditions were compared and analyzed. Based on the shakedown theory, the cumulative plastic deformation behavior and pore pressure characteristics of saturated sand under intermittent loading conditions were analyzed, and a combined predictive model for cumulative plastic strain was proposed with good prediction performance. The research findings are of great significance for understanding the deformation characteristics and long-term stability of sand filling and foundation under intermittent train loadings.

2 Dynamic triaxial tests

2.1 Experimental apparatus and soils

The experimental apparatus in this study is the DDS-70 microcomputer-controlled electromagnetic vibration triaxial testing system. It is comprised of measurement and control system, numerical adjustment system, confining pressure loading system, dynamic and static force loading system, as shown in Fig. 1.

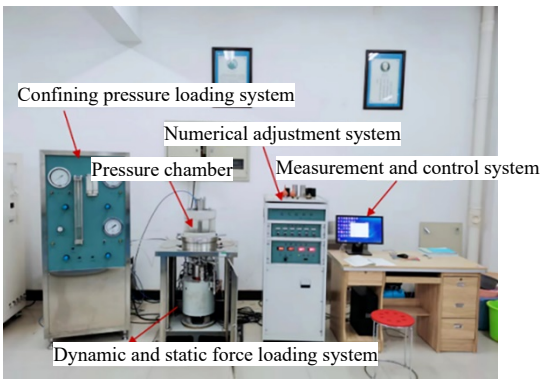

Fig. 1 DDS-70 dynamic triaxial testing system for soil

The apparatus exerts axial and lateral pressure through air pressure, while the measurement and control system records the force, displacement, and pore water pressure during the vibration process. The main parameters are as follows: maximum axial force of 1 372 N, loading frequency ranging from 1 to 10 Hz, maximum axial displacement of 20 mm, and lateral pressure between 0 and 600 kPa.

Sandy soil was employed to conduct sieve tests, relative compaction tests, and specific gravity test for soil particle. The obtained grading curve is shown in Fig. 2. The particle specific gravity G_s of the sand soil is 2.52, with a coefficient of uniformity (C_u) of 3.52 and a curvature coefficient (C_c) of 0.69. The maximum (e_{max}) and minimum (e_{min}) void ratios are 0.86 and 0.33, respectively. The maximum and minimum dry densities are 1.89 and 1.47 g /cm^3, respectively. Particles with a diameter greater than 0.5 mm account for 54.33% of the total mass, which is greater than 50%. According to Appendix A of *Code for design of subgrade and foundation of railway bridge and culvert* (TB10093−2017)[30], this type of sand can be classified as coarse sand.

2.2 Experimental parameters

The specimen size is 39.10 mm (diameter)×80 mm

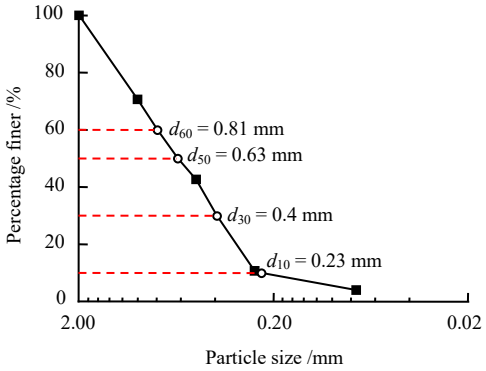

Fig. 2 Grain size distribution of tested soil

(height). The weight of each layer of soil sample is determined based on the pre-designed moisture content and dry density of the sand. After each layer was compacted to the corresponding height, the surface was scraped to prevent hierarchy. The preparation involved wet tamping in 5 layers, with a relative density (D_r) of 0.75. Saturation is achieved using the vacuum saturation method, with failure occurring when the axial strain reaches 10%.

Under both heavy-haul and subway train load conditions, the range of confining pressure on the subgrade (taking into account the embedment depth of the foundation) and filling materials is mainly between 0−150 kPa[8, 31]. Therefore, the confining pressure in the test was set at 50, 100, and 150 kPa.

Field tests and numerical analysis indicate that under the loading of trains with axle weights ranging from 13 to 35 t, the maximum dynamic stress range borne by the subgrade and foundation is between 20 and 300 kPa[27, 32−33]. To comprehensively analyze the three states of sandy soil ground and filling materials, including stability, criticality, and failure, intentional efforts were made to expand the range of dynamic stress amplitudes during testing, with values set between 30 and 400 kPa.

In actual railway and subway operations, vibrations from 8 to 240 times can be induced to the track and subgrade when a train passes through. For instance, when a 10 000 to 20 000 t train passes through, a fixed point in the subgrade and track endures 110 to 240 cyclic loads. In contrast, subways typically experience only 8 to 16 cyclic loads. To simulate more cycles of loading, the experimental loading phase was set to 200 cycles. Based on our previous research results[25] and field investigations, train intervals typically fluctuate within a range of 5 to 15 min with vibration cessation time set at between 5 to 15 min. Therefore, the experimental interval time was set at 900 s.

To determine the appropriate maximum vibration cycle, experiments were conducted under the conditions of confining pressure σ_3 = 100 kPa and dynamic amplitude σ_d = 30, 90, 120, and 240 kPa as well as 4 000 cycles. The variation of accumulated plastic strain with cycle number is shown in Fig. 3. Analysis reveals that the difference in accumulated plastic strain between 2 000 and 4 000 cycles is negligible, with differences of only 0.001%, 0.004%, 0.005%, and 0.02% for dynamic amplitudes of σ_d = 30, 90, 120, and 240 kPa, respectively. Therefore, the judgment and analysis of the variation trend of accumulated plastic strain are not affected by reducing the total number of cycles to N = 2 000. Considering the cost of experimentation, the total number of vibration cycles was set at N = 2 000.

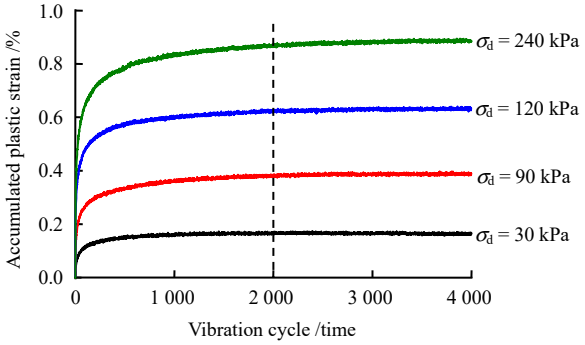

Fig. 3 Accumulated plastic strain-loading cycle (4 000) curve

Based on the results of field investigations of heavy-haul railways and subways, the typical speed of heavy-haul trains is between 60 and 80 km /h, with a carriage length of 12 to 14.9 m, corresponding to a frequency range of 1.39 to 1.85 Hz on the subgrade. The typical speed of subway trains is between 60 and 120 km /h, with a carriage length of 19 to 22.8 m, corresponding to a frequency range of 0.73 to 1.75 Hz on the subgrade. Therefore, a representative loading frequency of 1.5 Hz was set in testing.

2.3 Load simulation and test program

The stress-controlled method was used in experiments, with dynamic loads applied in the form of equal-amplitude sine waves. Based on the analysis in Section 2.2, two dynamic loading schemes were set up to compare the dynamic characteristics of sandy soil under continuous and intermittent loading conditions:

(1) Continuous loading. The loading process was undrained, with maximum vibration cycles of 2 000. The waveform of continuous loading is illustrated in Fig. 4(a).

(2) Intermittent loading. The loading process was divided into 10 loading stages, each with 200 cycles. After the loading was completed, the drainage valve at the bottom of the triaxial apparatus was opened to drain. When the intermittent time reaches 900 s, the drainage valve was closed and then load was exerted on the specimen again.

Loading and intermittent periods alternated until the end of the test, with a total duration of approximately 10 320 s. The waveform of intermittent loading is shown in Fig. 4(b).

The specific implementation program of the experiment is shown in Table 1.

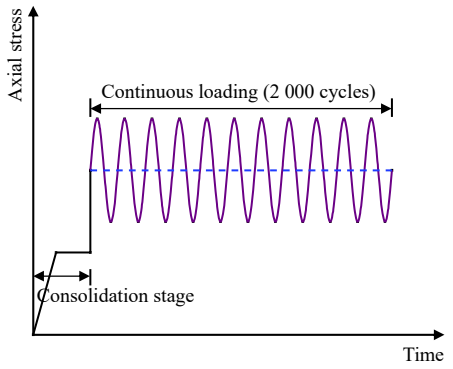

(a) Continuous loading

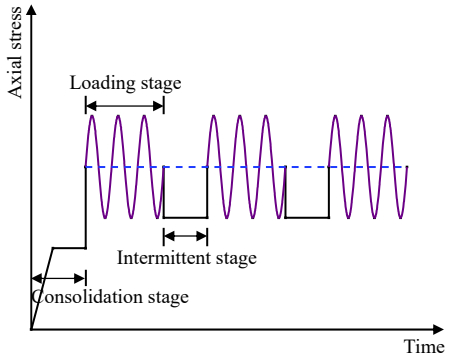

(b) Intermittent loading

Fig. 4 Loading patterns

Table 1 Dynamic triaxial test scheme

Loading patterns	Confining pressure σ_3 /kPa	Dynamic stress amplitude σ_d /kPa
Continuous loading (N = 2 000 cycles)	50	30，60，90，120
	100	30，60，90，120，240
	150	30，60，90，120，360
Intermittent loading (N = 200 cycles in each loading phase, with intermittent time of 900 s)	50	30，60，90，120，150
	100	30，90，120，240，270
	150	30，90，120，360，400

3 Experimental results and analysis

3.1 Effect of intermittent loading on accumulated plastic deformation

To comparatively analyze the accumulated plastic deformation characteristics under continuous and intermittent loading conditions, the relationship between accumulated plastic strain and loading cycle of the specimen under the same physical state and stress level is plotted in Fig. 5. To facilitate a direct comparison between the two loading conditions, the 900 s vibration-free stage after each level of intermittent loading will not be represented in the figure.

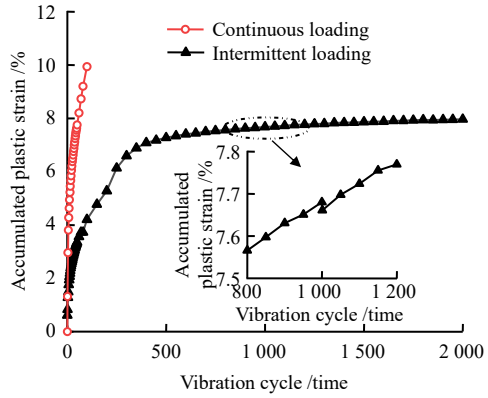

(a) The specimen under continuous loading to destroy and intermittent loading to stabilize (σ_3 = 50 kPa, σ_d = 120 kPa)

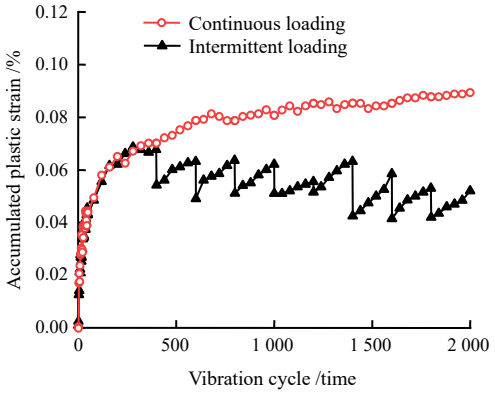

(b) The specimen that kept stable under both continuous and intermittent loading conditions (σ_3 = 50 kPa, σ_d = 120 kPa)

Fig. 5 Curves between accumulated plastic strain and loading cycle under different loading patterns

Figure 5(a) depicts the accumulated plastic strain curves of the specimen under continuous loading to destroy and intermittent loading to stabilize, with the conditions of σ_3 = 50 kPa and σ_d = 120 kPa. Analysis reveals that the accumulated plastic strain of the continuously loaded saturated sand soil increases rapidly with increasing number of cycles, reaching 9.8%, almost the failure point when N = 120 cycles. Under intermittent loading conditions, the accumulated plastic strain of the specimen increases rapidly in the first loading phase, experiences a period of vibration-free for 900 s, and then exhibits a significantly reduced growth rate in the second loading phase. After another period of vibration-free, the subsequent accumulated plastic strain tends to be gradual, ultimately reaching a value of 7.9%. Compared to the failure state under continuous loading conditions, the specimen under intermittent loading maintains a stable state. Therefore, it can be concluded that the existence of intermittent phases significantly improves the resistance of sand soil to failure.

Figure 5(b) displays the accumulated plastic strain

curves of specimens that kept stable under both continuous and intermittent loading conditions, with stress levels of σ_3 = 150 kPa and σ_d = 30 kPa, respectively. The accumulated plastic strain of the specimen under continuous loading reaches 0.09% after 2 000 cycles, while that of the specimen under intermittent loading reaches a final value of 0.05%, indicating a reduction in accumulated plastic strain by 43% due to the presence of intervals. Moreover, the subsequent single loading stages exhibit a decrease in accumulated plastic strain due to the drainage consolidation effect during the intervals, which densifies the sand soil specimen and leads to a reduction in accumulated plastic strain during the next vibration stage.

In summary, it can be concluded that there are significant differences in the development of accumulated plastic deformation in sand soil under continuous and intermittent loading conditions.

3.2 Effect of intermittent loading on excess pore water pressure

To investigate the variation of excess pore water pressure with loading cycles under continuous and intermittent loading conditions, and to reveal the mechanism of accumulated plastic deformation characteristics, a relationship curve of excess pore water pressure versus loading cycles is displayed in Fig. 6.

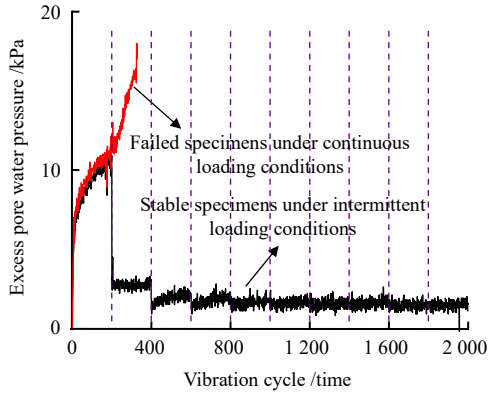

(a) σ_3 = 50 kPa, σ_d = 120 kPa

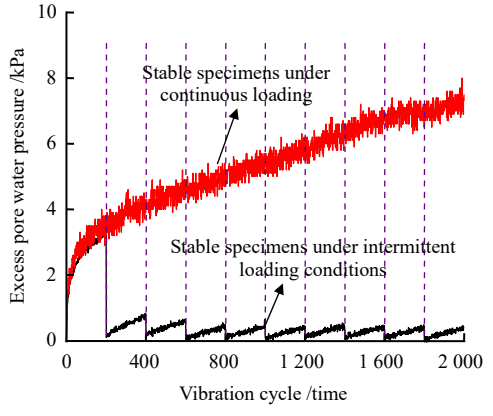

(b) σ_3 = 150 kPa, σ_d = 120 kPa

Fig. 6 Excess pore water pressure versus loading cycles

Figure 6(a) depicts the relationship between excess pore water pressure and number of cycles for a continuously loaded specimen that failed and a cyclically loaded specimen that remained stable under the conditions of σ_3 = 50 kPa and σ_d = 120 kPa. Analysis of Fig. 6(a) reveals that, under continuous loading, excess pore water pressure in the sample increases rapidly with increasing number of cycles, and the sample fails after 360 cycles. Under intermittent loading conditions, the first stage exhibits a rapid increase in excess pore water pressure, while in the intermittent stage, pore pressure dissipates and decreases. In the second loading stage, pore pressure slowly accumulates with increasing cycles, but the amplitude of the increase is greatly reduced. In subsequent loading stages, the accumulated amplitude of excess pore water pressure decreases continuously with an increasing number of loading stages and approaches a stable value of 1.5 kPa, which is only 3.3% of the value under continuous loading. Combining this with Fig. 5(a), it can be concluded that unloading and dissipation of pore water pressure in intermittent phases raise effective stress between particles and the compactness of the specimen, enhancing dynamic stability of sand soil subjected to cyclic loads. Hence, the dissipation effects of unloading and excess pore water pressure in the intermittent period can alter the variation trend and type of accumulated plastic deformation (from destructive to stable).

Figure 6(b) illustrates the excess pore water pressure−cycle relationship of stable specimens under both continuous and intermittent loading conditions at a stress condition of σ_3 = 150 kPa and σ_d = 120 kPa. Under continuous loading, the excess pore water pressure of the specimen increases rapidly with increasing cycles when N is between 0 and 200. When N is between 200 and 2 000 cycles, the excess pore water pressure gradually accumulates with increasing cycles, and the rate of increase remains relatively constant. At N = 2 000 cycles, the excess pore water pressure reaches 8 kPa, which is much smaller than the confining pressure, and the sample remains stable. Under intermittent loading conditions, the growth pattern of excess pore water pressure in the first loading stage is consistent with that under continuous loading conditions. However, due to drainage and unloading in the intermittent stage, the accumulation of excess pore water pressure in the loading stage decreases close to zero. In the next loading stage, the excess pore water pressure will accumulate again, but its maximum value decreases with increasing loading cycles. The final value of excess pore water pressure under intermittent loading is only 0.5 kPa, which is 1/16 of that under continuous loading. The existence of the intermittent stage significantly reduces the accumulation

of excess pore water pressure in the sample.

3.3 Analysis of plastic deformation behavior during intermittent loading

To analyze the overall variation of accumulated plastic strain with increasing cycles under different confining pressures and dynamic stress amplitudes, the curve of accumulated plastic strain versus loading cycle of saturated sand soil under different confining pressure conditions is plotted in Fig. 7. The data points were selected based on the following criteria: for the first loading stage, data points were taken at intervals of 5 cycles for N = 0−50 cycles and at intervals of 50 cycles for N = 50−200 cycles; for loading stages 2−10, data points were taken at intervals of 50 cycles.

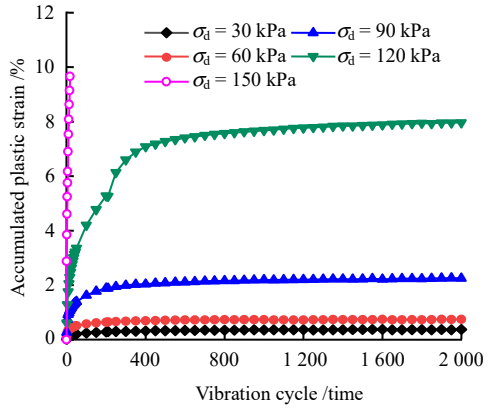

(a) σ_3 = 50 kPa

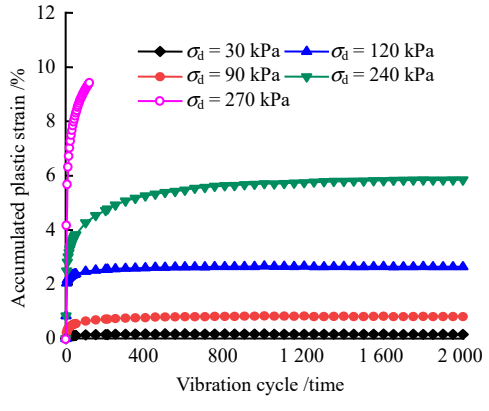

(b) σ_3 = 100 kPa

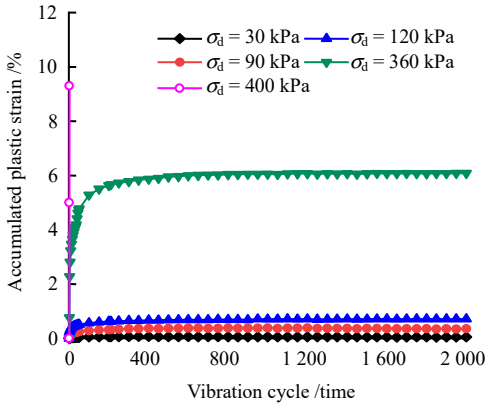

(c) σ_3 = 150 kPa

Fig. 7 Curves between accumulated plastic strain and loading cycle under intermittent loading

According to Fig. 7, it is evident that the dynamic stress amplitude σ_d has a significant impact on the development of accumulated plastic strain. The condition σ_3 = 50 kPa is presented as an example(see Fig. 7(a)). An analysis of the variation of accumulated plastic strain reveals that:

(1) With dynamic stress amplitude of σ_d = 30, 60, and 90 kPa, the accumulated plastic strain rapidly increases in the first loading stage and then tends to stabilize. At the end of the first loading stage, the accumulated plastic strains are 0.28%, 0.64%, and 1.88%, respectively. When the sample is loaded for 2 000 cycles, the accumulated plastic strains are 0.37%, 0.74%, and 2.18%, respectively, which have increased by 32%, 16%, and 16% as compared to those at the end of the first loading stage. The samples remain stable.

(2) With dynamic stress amplitude of σ_d = 120 kPa, the accumulated plastic strain increases rapidly in both the first and second loading stages. At the end of the second loading stage, the accumulated plastic strain is 7.08%. When loaded for 2 000 cycles, it increases to 7.9% by 12%. The sample remains in a stable state at the end of loading.

(3) With dynamic stress amplitude of σ_d = 150 kPa, the accumulated plastic strain rapidly increases in the first loading stage and reaches the termination criterion. It is evident that an increase in dynamic stress amplitude significantly enhances accumulated plastic strain.

When the confining pressure is increased to 100 kPa and 150 kPa, the variation of accumulated plastic deformation with increasing loading cycles follows a similar pattern as that under a confining pressure of 50 kPa. However, as the confining pressure increases, the dynamic stress amplitude to failure due to accumulated plastic deformation also increases.

The relationship between accumulated plastic strain and confining pressure is illustrated in Fig. 8. It reveals that under the same dynamic stress, the accumulated plastic strain of the specimen decreases as confining pressure increases, but the decreasing rate narrows. Figure 9 illustrates the relationship between accumulated plastic strain and dynamic stress amplitude. It can be found that under the same confining pressure, the accumulated plastic strain of the specimen increases rapidly with an increase in dynamic stress amplitude.

Currently, the concept of shakedown is widely used to describe the permanent deformation characteristics of granular materials under repeated dynamic loads[34−35], and its applicability has been widely recognized. Based on the shakedown concept, the plastic deformation behavior

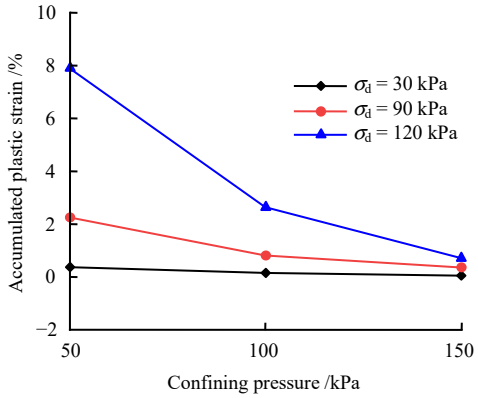

Fig. 8 Cumulative plastic strain versus confining pressure

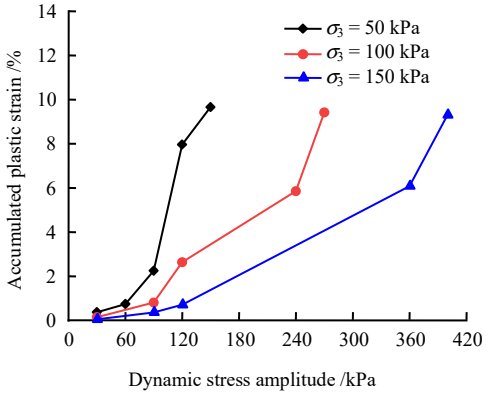

Fig. 9 Cumulative plastic strain versus dynamic stress amplitude

of sand soil under intermittent loading can be divided into three ranges: plastic shakedown (Range A), plastic creep (Range B), and incremental failure (Range C). According to the aforementioned variation of accumulated plastic strain, the description of plastic shakedown behavior in the shakedown theory is that plastic deformation only accumulates at the initial loading stage. With an increase in loading cycles, the rate of plastic deformation decreases rapidly to a low level or even zero, and eventually, and the specimen enters a stable state[36−37]. Figure 10 shows the curve of accumulated plastic strain and strain rate with loading cycles for specimens in a state of plastic shakedown.

Figure 10(a) indicates that for specimens in a plastic stable state, the accumulated plastic strain can be divided into the following stages. Stage 1 — rapid increase, corresponding to the first loading stage, N = 0−200 cycles. Stage 2 — slow growth, corresponding to the second loading stage, N = 200−400 cycles. Stage 3 — stable stage, where the accumulated plastic strain at the end of the second loading stage is close to that at the end of the test. In subsequent loading stages, plastic strain remains nearly constant. Figure 10(b) reveals that after the first loading stage, there is a significant decrease in plastic strain rate. As loading stages increase (second, third or fourth), the plastic strain rate of specimens further decreases to a low level (5.05×10^{-6}% /cycle−8.18×10^{-5}% /cycle), and remains stable in subsequent stages.

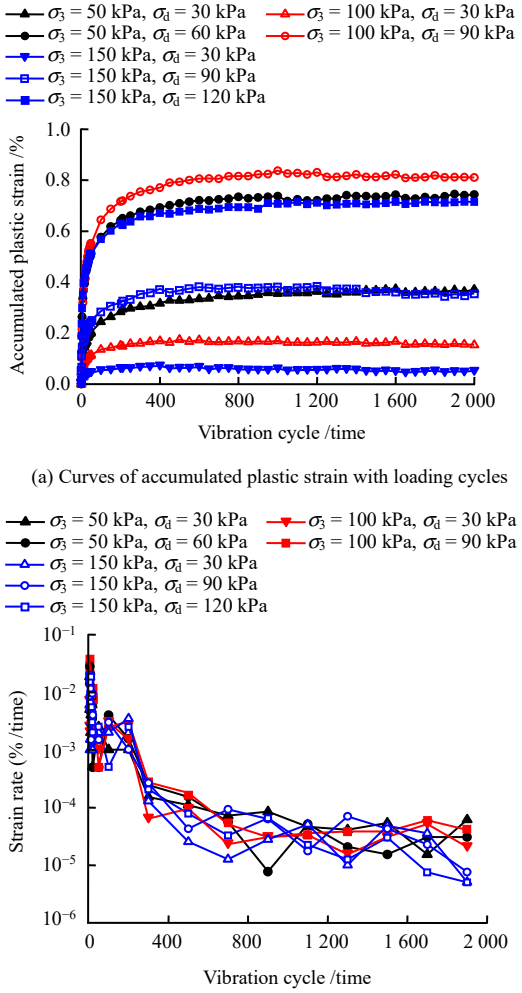

(a) Curves of accumulated plastic strain with loading cycles

(b) Curves of strain rate with loading cycles

Fig. 10 Accumulated plastic strain and its rate with loading cycles in Range A

The description of plastic creep behavior in the shakedown theory states as follows: The accumulated plastic strain increases continuously with the increase of loading cycles, and although the plastic strain rate decreases with the increase of loading cycles, it still remains at a certain level. The final accumulated plastic deformation of the specimen is relatively large and tend to continuously increase[36−37]. Figure 11 shows the curves of accumulated plastic strain and strain rate with loading cycles for specimens under plastic creep conditions. Figure 11(a) indicates that for specimens under plastic creep conditions, their accumulated plastic strain rapidly develops to a certain level in the early stage of loading and then increases slowly. Figure 11(b) shows that due to intermittent stages, the accumulated plastic strain rate of specimens decreases rapidly. However, compared with specimens under stable plastic conditions, the subsequent accumulated plastic

strain rate still remains at a relatively high level, ranging from 9.3×10^{-5}% /cycle to 4.65×10^{-4}% /cycle. At the end of the test, the accumulated plastic strain is still increasing.

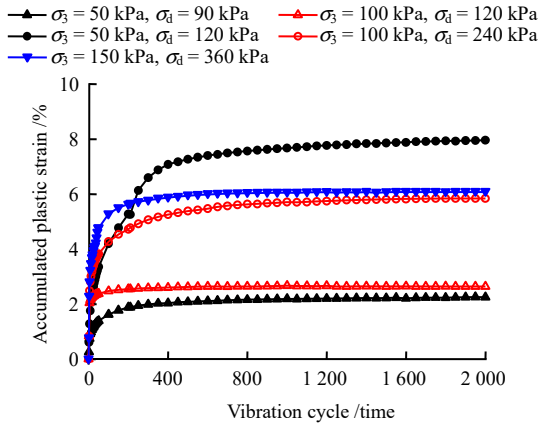

(a) Curves of accumulated plastic strain with loading cycles

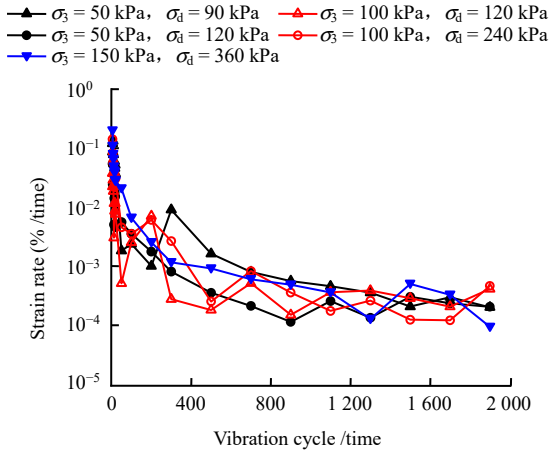

(b) Curves of strain rate with loading cycles

Fig. 11 Accumulated plastic strain and its rate with loading cycles in Range B

Figure 12 displays the variation of accumulated plastic strain and strain rate with the number of loading cycles for specimens in an incremental damaged state. Figure 12(a) indicates that the accumulated plastic strain of the specimen in an incremental damaged state rapidly increases until failure during the initial loading cycles (N = 0−200). Figure 12(b) shows that although the strain rate decreases with increasing cycles, it remains at a high level (not less than 5×10^{-3}% /cycle) overall. Eventually, the specimen fails due to excessive accumulated plastic strain.

3.4 Analysis of pore pressure characteristics under intermittent loading

The curves of excess pore water pressure of saturated sandy soil under different confining pressures with respect to loading cycles is presented in Fig. 13. The relationship between excess pore water pressure, and confining pressure as well as dynamic stress amplitude after the first loading stage is depicted in Fig. 14. Analysis of Figs. 13 and 14 reveals that:

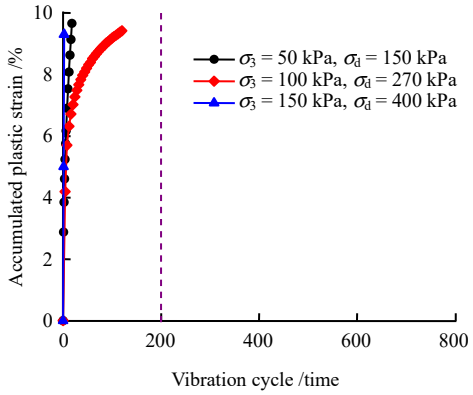

(a) Curves of accumulated plastic strain with loading cycles

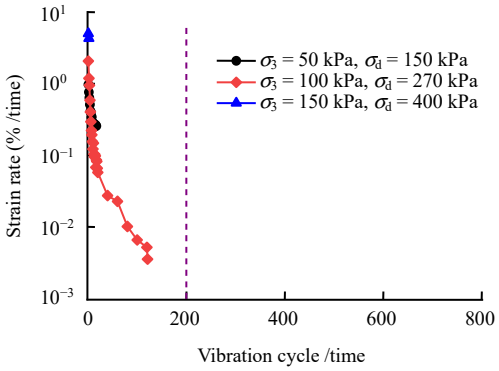

(b) Curves of strain rate with loading cycles

Fig. 12 Accumulated plastic strain and its rate with loading cycles in Range C

(1) During the first loading stage, the excess pore water pressure of all specimens increases rapidly with increasing cycles. During the intermittent period, the excess pore water pressure approaches or decreases to zero due to drainage of the specimen. Moreover, in subsequent loading stages, the accumulated excess pore water pressure decreases significantly and is much smaller than that in the first loading stage.

(2) Under the same confining pressure conditions, the greater the amplitude of dynamic stress, the greater the accumulated increase in pore pressure. This effect is most pronounced during the first loading stage, but diminishes as loading stages increase.

(3) Under the same conditions of dynamic stress amplitude, a higher confining pressure results in a smaller increase in pore water pressure.

Based on the above analysis, it is evident that the presence of intermittent stages significantly affects the long-term dynamic response of saturated sandy soil. Under continuous loading conditions, the experimental pore pressure accumulates continuously, resulting in the accumulation of accumulated plastic strain with loading cycles. Intermittent stages can reduce the accumulation of pore pressure and strain in saturated sandy soil, altering the characteristics of plastic deformation behavior under

continuous loading conditions from a failure-type to a stable-type. When studying the dynamic response of saturated sandy soil foundations or filling materials under train loadings, continuous loading underestimates their dynamic strength to some extent.

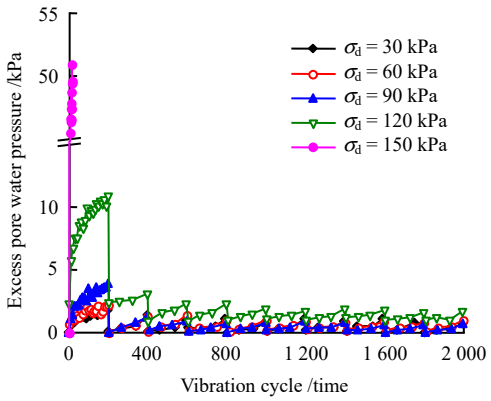

(a) σ_3 = 50 kPa

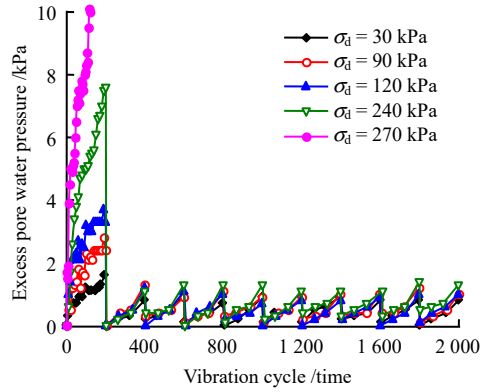

(b) σ_3 = 100 kPa

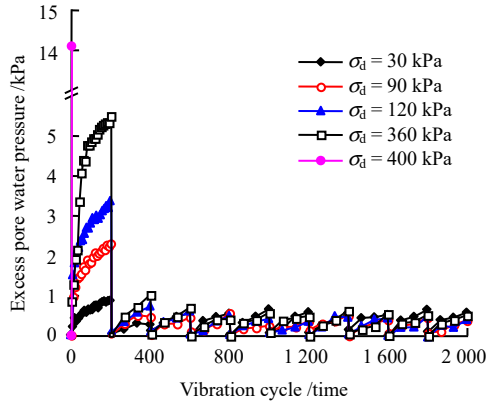

(c) σ_3 = 150 kPa

Fig. 13 Excess pore water pressure versus loading cycles under intermittent loading

4 A model to predict accumulated plastic strain

The commonly used expressions for the prediction of accumulated plastic strain for granular materials under repeated dynamic loads and their features are listed in Table 2.

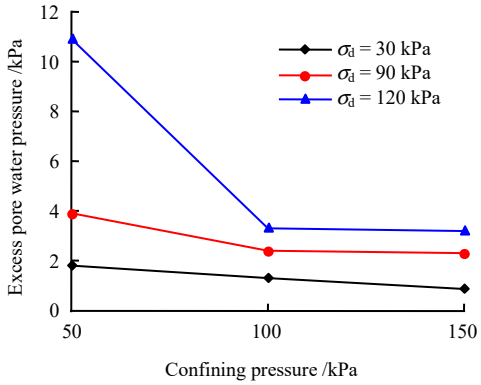

(a) Confining pressure

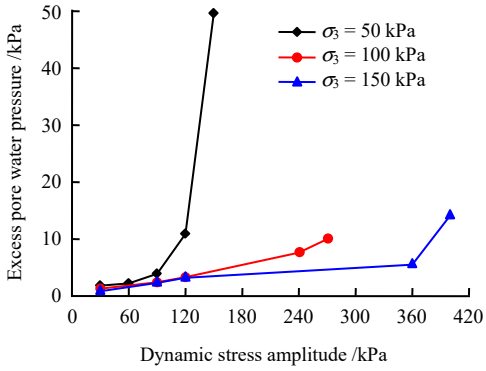

(b) Dynamic stress amplitude

Fig. 14 Pore water pressure versus confining pressure and dynamic stress amplitude

Based on Fig. 7, the development of accumulated plastic strain in the sand soil specimen can be divided into two stages: (1) The stage of rapid increase in initial densification and accumulated plastic strain ($N \leqslant N_0$). During the initial loading stage, the growth rate of accumulated strain is relatively high, but it decreases rapidly with increasing number of loading cycles. This phenomenon has also been observed in the experimental results by Lekarp et al.[45]. (2) The stage of slow increase in cyclic densification and accumulated plastic strain. The characteristic of this stage is that the strain rate is small (9.3×10^{-5}% /cycle to 4.65×10^{-4}% /cycle). Therefore, to better characterize and describe the different development characteristics of accumulated plastic strain in these two stages, Model 6 from Table 2 is selected as the predictive model for accumulated plastic strain. By combining the experimental results presented in this paper, for intermittent loading, the first continuous loading stage can be considered as an initial densification stage, and the number of repeated

cycles N at the end of loading is referred to as N_0. After the first interval, the accumulated plastic strain enters a slow-development stage. Therefore, the threshold value N_0 between the two stages is set as 200.

Table 2 Common accumulated plastic strain models

No.	Models	Refs.	Note
1	$\varepsilon_p = a + b\lg N$	Barksdale[38]	The model has a concise form and is easy to determine parameters, but the continuous increase of permanent accumulated strain does not match the actual stable subgrade.
2	$\varepsilon_p = aN^b$	Monismith et al.[39]	These parameters are inadequate in describing the stress state and physical properties of the roadbed.
3	$\varepsilon_p = \dfrac{N^c}{a + bN^c}$	Zhang et al.[40]	It is unable to depict the history of stress.
4	$\varepsilon_p = a\left(\dfrac{q_d}{q_f}\right)^m \left(1+\dfrac{q_s}{q_f}\right)^n N^b$	Chai et al.[41]	It cannot adequately represent the history of stress.
5	$\varepsilon_p = \varepsilon^0\left[1-\left(\dfrac{N}{100}\right)^{-B}\right]\left(\dfrac{L_{max}}{p_a}\right)\left(m+\dfrac{s}{p_{max}}-\dfrac{q_{max}}{p_{max}}\right)$	Gidel et al.[42]	—
6	$\varepsilon_{1,p}(N) = \varepsilon^0_{1,p}(100) + \varepsilon^*_{1,p}(100)$ $\varepsilon^0_{1,p}(N) = a_1\left(\dfrac{N}{100}\right)^{b_1}$ $\varepsilon^*_{1,p} = a_2\left[1-\left(\dfrac{N}{100}\right)^{-b_2}\right]$	Paute[43], Nie[44] et al.	Two-stage fitting for initial compaction and secondary cyclic compression phase

Where q_d is the dynamic stress amplitude, q_s is the static deviatoric stress, q_f is the static strength, N is the loading cycle, p_a is the standard atmospheric pressure, L_{max} is the stress path length, p_{max} and q_{max} are the maximum average stress and maximum deviatoric stress, $\varepsilon_{1,p}$ is the accumulated plastic strain, and a, b, c, a_1, b_1, a_2, b_2, s, m, n, ε^0 and B are all fitting parameters.

$$\varepsilon_p(N) = \begin{cases} A_1\left(\dfrac{N}{200}\right)^{B_1}, 0 \leqslant N \leqslant 200 \\ \varepsilon_p(200) + A_2\left[1-\left(\dfrac{N}{200}\right)^{-B_2}\right], N > 200 \end{cases} \quad (1)$$

where $\varepsilon_p(N)$ represents the total accumulated plastic strain of the specimen; $\varepsilon_p(200)$ represents the plastic strain generated in the first 200 cycles; and A_1, B_1, A_2, and B_2 are regression parameters, all of which are greater than 0.

Using Eq. (1), the measured data of accumulated plastic strain under creep conditions in Fig. 11 were fitted and shown in Fig. 15. The regression parameters and correlation coefficient R^2 values for the plastic strain prediction model of saturated sand soil under three confining pressure conditions are summarized in Table 3. Analyzing Fig. 15 and Table 3 reveals that the average R^2 is 0.963, indicating a high correlation between the predicted results of the model and experimental data. This demonstrates that the adopted prediction model is reliable and consistent with the experimental data.

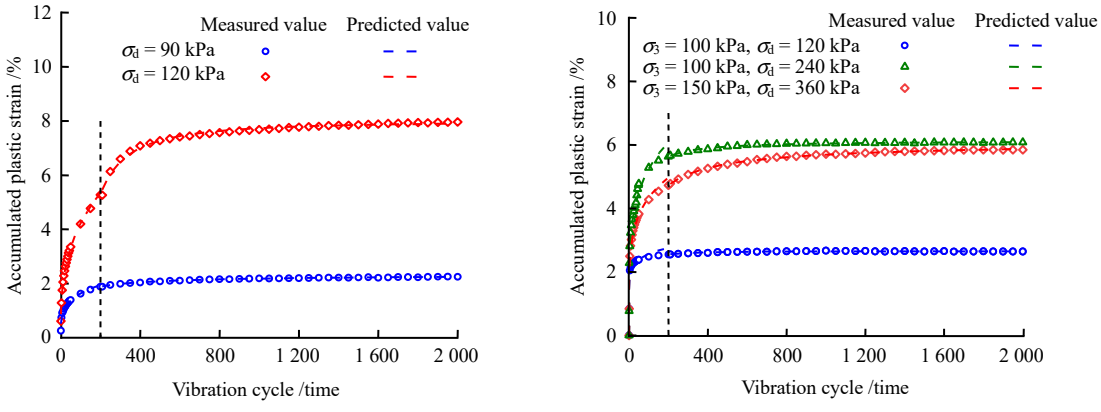

(a) σ_3 = 50 kPa (b) σ_3 = 100、150 kPa

Fig. 15 Prediction results of cumulative plastic strain

Table 3 Regression parameters for prediction model

σ_3 /kPa	σ_d /kPa	$\varepsilon_p^0(N)=A_1\left(\frac{N}{200}\right)^{B_1}$ (0≤N≤200)		R^2	$\varepsilon_p^*=A_2\left[1-\left(\frac{N}{200}\right)^{B_2}\right]$ (N>200)		R^2
		A_1	B_1		A_2	B_2	
50	90	2.316	0.250	0.965	0.504	0.561	0.995
	120	6.765	0.342	0.995	2.723	1.445	0.987
100	120	2.759	0.106	0.890	0.109	1.407	0.918
	240	4.965	0.194	0.952	1.443	0.689	0.997
150	360	6.081	0.214	0.950	0.496	1.076	0.982

5 Conclusions

(1) Under intermittent loading, the curve of accumulated plastic deformation of saturated sand soil with loading cycles exhibits a "sawtooth" variation tendency. During the intermittent stage, unloading-induced rebound and drainage dissipate the excess pore water pressure accumulated during the previous loading stage, compacting the soil and significantly reducing the accumulation of plastic deformation and pore water pressure during subsequent loading stages. This enhances the ability of sand soil to resist accumulated plastic deformation and can transform its plastic deformation behavior from a destructive type to a stable type under continuous loading conditions.

(2) Under intermittent loading, the overall relationship between the excess pore water pressure and the number of cycles for saturated sand soil exhibits a step-like variation trend. For plastic-stable and plastic-creep types, the excess pore water pressure during the first loading stage rapidly increases with the number of cycles, while during the intermittent period, the pore pressure approaches or decreases to zero. In subsequent loading stages, the accumulated amplitude of pore pressure significantly decreases and is much smaller than that of the first loading stage. For incremental failure type, pore pressure rapidly increases during the first loading stage until failure occurs. Excess pore water pressure decreases with increasing confining pressure but increases with increasing dynamic stress amplitude.

(3) A predictive model was established to characterize the two-stage accumulated plastic strain in saturated sand soil under intermittent loading. The fitting results of the model were in good agreement with experimental data, verifying its reliability.

(4) The intermittent effect enhances the resistance of sand soil to plastic deformation. Simulating train loads using continuous loading overestimates the accumulated plastic strain and underestimates the dynamic strength of saturated sand soil. The research results provide important reference value for a profound understanding of the accumulated deformation characteristics and mechanisms of saturated sand soil under intermittent cyclic loading, and can provide a theoretical basis for assessing the accumulated settlement deformation of saturated sand soil subgrade under long-term train loads.

References

[1] XU Bin. Experimental study on liquefaction and behavior of post-liquefaction deformation and strength in saturated sand-gravel composites[D]. Dalian: Dalian University of Technology, 2007.

[2] WANG Xiu-ying, LIU Wei-ning. Study of the possibility of sand liquefaction of the immersed tube tunnel under train vibration[J]. Journal of the China Railway Society, 2004, 26(1): 96−100.

[3] DAI Lin-fa-bao, WANG Guang-di, GAO Bo. Study of sand liquefaction under vibration load of high speed train[J]. Chinese Journal of Underground Space and Engineering, 2012, 8(2): 434−438.

[4] GONG Quan-mei, ZHOU Shun-hua, WANG Bing-long. Variation of pore pressure and liquefaction of soil in metro[J]. Chinese Journal of Geotechnical Engineering, 2004, 26(2): 290−292.

[5] YE Wei-tao, FU Long-long, SHAN Yao, et al. Experimental study on dynamic characteristics of granular materials under axial high-frequency vibration[J]. Acta Geotechnica, 2022, 17: 3211−3227.

[6] YANG Xiu-zhu, WANG Xing-hua, LEI Jin-shan. Study on dynamic characteristics of Xiangjiang saturated sand under isobaric consolidation[J]. Journal of Vibration and Shock, 2007, 26(9): 146−148.

[7] CHANG Shi-qing, BAI Hai-feng, YE Jian-hong, et al. Dynamic response of railway sandy foundation under train running loading[J]. Journal of Engineering Geology, 2014, 22(6): 1077−1085.

[8] LU Shan-jia, XUE Ting, WANG Xu-dong, et al. Distribution characteristics of excess pore water pressure and power cumulative settlement regularity of dynamic load under various operation modes of subway[J]. Journal of Nanjing University of Technology (Natural Science Edition), 2013, 35(5): 94−99.

[9] WANG Tao, SHI Bin, MA Long-xiang, et al. Dynamic response and long-term cumulative deformation of silty sand stratum induced by metro train vibration loads[J]. Journal of Engineering Geology, 2020, 28(6): 1378−1385.

[10] LIU Jun-lin. Dynamic characteristics of saturated sandy soil foundation under vibration load of high speed rail[D]. Xuzhou: China University of Mining and Technology, 2019.

[11] CERNI G, CARDONE F, VIRGILI A. Characterisation of permanent deformation behaviour of unbound granular materials under repeated triaxial loading[J]. Construction and Building Materials, 2012, 28(1): 79−87.

[12] VAID Y P, CHERN J C. Effect of static shear on resistance to liquefaction[J]. Soils and Foundations, 1983, 23(1): 47−60.

[13] LIU Kai, ZHANG Yuan-fang. Study on dynamic pore water pressure characteristics of saturated fine gravel sand by triaxial test[J]. Science Technology and Engineering, 2016, 16(19): 283−287.

[14] QIAN Ming. Dynamic triaxial test of saturated fine sand liquefaction potential[J]. Journal of Chengdu University (Natural Science Edition), 2015, 34(4): 408−411.

[15] ZHANG Su, ZHANG Yuan-fang, ZHANG Ling-kai, et al. Influence of confining pressure and vibration frequency on the liquefaction strength of the saturated gravel sand[J].

Journal of Xinjiang Agricultural University, 2015, 38(1): 68−71.

[16] PADHAN S K, DESAI C S. DSC model for soil interface including liquefaction and prediction of centrifuge test[J]. Journal of Geotechnical and Geoenvironmental Engineering, 2006, 132(2): 214−222.

[17] WANG Jia. Experimental study on dynamic elasticity modulus and damping ratio of coarse-grained soils[D]. Changsha: Central South University, 2013.

[18] LIU Da-peng, YANG Xiao-hua, WANG Jing, et al. Study on influence factors of gravel soil accumulative deformation under cyclic loading[J]. Journal of Railway Science and Engineering, 2014, 11(4): 68−72.

[19] CHANG Zhen-chao, WANG Jia-quan, ZHOU Yuan-wu, et al. Dynamic triaxial test analysis of gravel soil under traffic dynamic load[J]. Journal of Guangxi University of Science and Technology, 2019, 30(2): 13−19.

[20] YILMAZ Y, MOLLAMAHMUTOGLU M. Characterization of liquefaction susceptibility of sands by means of extreme void ratios and/or void ratio range[J]. Journal of Geotechnical and Geoenvironmental Engineering, 2009, 135(12): 1986−1990.

[21] PUMPHREY N D, LENTZ R W. Deformation analyses of Florida highway subgrade sand subjected to repeated load triaxial tests[J]. Transportation Research Record, 1986, 1089: 49−56.

[22] TANG L, YAN M H, LING X Z, et al. Dynamic behaviours of railway's base course materials subjected to long-term low-level cyclic loading: experimental study and empirical model[J]. Geotechnique, 2017, 67(6): 537−545.

[23] SALOUR F, ERLINGSSON S. Permanent deformation characteristics of silty sand subgrades from multistage RLT tests[J]. International Journal of Pavement Engineering, 2017, 18(3-4): 236−246.

[24] HUANG Bo, DING Hao, CHEN Yun-min. Simulation of high-speed train load by dynamic triaxial tests[J]. Chinese Journal of Geotechnical Engineering, 2011, 33(2): 195−202.

[25] LI Ya-feng, NIE Ru-song, LI Yuan-jun, et al. Cumulative plastic deformation of subgrade fine-grained soil under intermittent cyclic loading and its prediction model[J]. Rock and Soil Mechanics, 2021, 42(4): 1065−1077.

[26] LI Ya-feng, NIE Ru-song, LENG Wu-ming, et al. Deformation characteristics of fine-grained soil under cyclic dynamic loading with intermittence[J]. Journal of Zhejiang University (Engineering Science), 2020, 54(11): 2109−2119.

[27] NIE Ru-song, DONG Jun-li, MEI Hui-hao, et al. Dynamic characteristics of silt considering time intermittent effect[J]. Journal of Southwest Jiaotong University, 2021, 56(5): 1125−1134.

[28] WANG Jun, CAI Yuan-qiang, GUO Lin, et al. Pore pressure and strain development of Wenzhou saturated soft soil under cyclic loading by stages[J]. Chinese Journal of Geotechnical Engineering, 2012, 34(7): 1349−1354.

[29] YILDIRIM H, ERSAN H. Settlements under consecutive series of cyclic loading[J]. Soil Dynamics and Earthquake Engineering, 2007, 27(6): 577−585.

[30] China Railway Design Corporation. TB 10093—2017 Code for design on subsoil and foundation of railway bridge and culvert[S]. Beijing: China Railway Publishing House, 2017.

[31] NIE Ru-song, LI Ya-feng, LENG Wu-ming, et al. Plastic deformation behavior and critical dynamic stress of fine-grained soil under intermittent loading of trains[J]. Chinese Journal of Rock Mechanics and Engineering, 2021, 40(4): 828−841.

[32] YANG Qi, ZHANG Lei, WEI Li-min, et al. Probability distribution law and value of dynamic stress amplitude on subgrade surface under high-speed railway train load[J]. China Civil Engineering Journal, 2022, 55(9): 78−93.

[33] LI Zi-chun. Study on the vertical load transmision through the track structure and the characteristics of subgrade dynamic stress[D]. Beijing: China Academy of Railway Sciences, 2000.

[34] WERKMEISTER S, DAWSON A, WELLNER F. Permanent deformation behavior of granular materials and the shakedown concept[J]. Journal of the Transportation Research Board, 2001, 1757(1): 75−81.

[35] WERKMEISTER S, DAWSON A R, WELLNER F. Pavement design model for unbound granular materials[J]. Journal of Transportation Engineering, 2004, 130(5): 665−674.

[36] WERKMEISTER S. Permanent deformation behavior of unbound granular materials in pavement construction[D]. Dresden: Dresden University of Technology, 2003.

[37] DAWSON A R, WELLNER F. Plastic behavior of granular materials[R]. Nottingham: University of Nottingham, 1999.

[38] BARKSDALE R D. Laboratory evaluation of rutting in base course materials[C]//The Third International Conference on the Structural Design of Asphalt Pavements. London: Grosvenor House, 1972: 11−15.

[39] MONISMITH C L, OGAWA N, FREEME C R. Permanent deformation characteristics of subgrade soils due to repeated loading[J]. Transport Research Record, 1975, 537: 1−17.

[40] ZHANG Yong, KONG Ling-wei GUO Ai-guo, et al. Cumulative plastic strain of saturated soft clay under cyclic loading[J]. Rock and Soil Mechanics, 2009, 30(6): 1542−1548.

[41] CHAI J C, MIURA N. Traffic loading induced permanent deformation of road on soft subsoil[J]. Journal of Geotechnical and Geoenvironmental Engineering, 2002, 128(11): 907−916.

[42] GIDEL G, HORNYCH P, CHAUVIN J, et al. A new approach for investigating the permanent deformation behaviour of unbound granular material using the repeated loading triaxial apparatus[J]. Bulletin de Liaison des Laboratoires des Ponts et Chaussees, 2001, 233: 5−21.

[43] PAUTE J L, HORNYCH P, BENABEN J P. Repeated load triaxial testing of granular materials in the French Network of Laboratories des Ponts et Chaussees[C]//Proceedings of the European Symposium Euroflex Lisbon. Portugal: A A Balkema, 1996: 53−64.

[44] NIE Ru-song, MEI Hui-hao, LENG Wu-ming, et al. Characterization of permanent deformation of fine-grained subgrade soil under intermittent loading[J]. Soil Dynamics and Earthquake Engineering, 2020, 139: 106395.

[45] LEKARP F, RICHARDSON I R, DAWSON A. Influences on permanent deformation behavior of unbound granular materials[J]. Transportation Research Record, 1996, 1547(1): 68−75.